



NRL/MR/5621--98-8184

December 1996

Field Test of the Fiber Optic Infrared Cone Penetrometer

F. BUCHOLTZ
G.M. NAU
G.H. HAZEL
K.J. EWING
J.A. McVICKER
I.D. AGGARWAL

*Fiber Optic Environmental Sensor Section
Optical Sciences Division*

July 31, 1998

19980729 010

Approved for public release; distribution is unlimited.

REPORT DOCUMENTATION PAGE

Form Approved
OMB No. 0704-0188

Public reporting burden for this collection of information is estimated to average 1 hour per response, including the time for reviewing instructions, searching existing data sources, gathering and maintaining the data needed, and completing and reviewing the collection of information. Send comments regarding this burden estimate or any other aspect of this collection of information, including suggestions for reducing this burden, to Washington Headquarters Services, Directorate for Information Operations and Reports, 1215 Jefferson Davis Highway, Suite 1204, Arlington, VA 22202-4302, and to the Office of Management and Budget, Paperwork Reduction Project (0704-0188), Washington, DC 20503.

1. AGENCY USE ONLY (<i>Leave Blank</i>)	2. REPORT DATE July 31, 1998	3. REPORT TYPE AND DATES COVERED	
4. TITLE AND SUBTITLE December 1996 Field Test of the Fiber Optic Infrared Cone Penetrometer		5. FUNDING NUMBERS	
6. AUTHOR(S) F. Bucholtz, G.M. Nau, G.H. Hazel, K.J. Ewing, J.A. McVicker, and I.D. Aggarwal			
7. PERFORMING ORGANIZATION NAME(S) AND ADDRESS(ES) Naval Research Laboratory Washington, DC 20375-5320		8. PERFORMING ORGANIZATION REPORT NUMBER NRL/MR/5621--98-8184	
9. SPONSORING/MONITORING AGENCY NAME(S) AND ADDRESS(ES) Commander U.S. Army Environmental Center SFIM-AEC-ETD Aberdeen Proving Grounds, Maryland ATTN: Mr. George Robitaille		10. SPONSORING/MONITORING AGENCY REPORT NUMBER	
11. SUPPLEMENTARY NOTES			
12a. DISTRIBUTION/AVAILABILITY STATEMENT Approved for public release; distribution unlimited.		12b. DISTRIBUTION CODE	
13. ABSTRACT (<i>Maximum 200 words</i>) A two-day field test of NRL's fiber optic infrared cone penetrometer was conducted at a site suspected of containing shallow deposits of chlorinated solvents. The electro-optical system, including recent improvements, worked nominally throughout the test. Laboratory characterization of the system demonstrated the capability to detect and identify 1,2 DCA, 1,1 DCA and TCE at weight fractions greater than 2 wt% in sample soil taken from the test site containing 20 wt% water. No evidence of homogeneously-distributed, free-product DNAPL in excess of 2 wt% was observed. In it's current form, the fiber optic infrared cone penetrometer is suitable for identifying contaminants in saturated, free-product pools in known locations. Further improvements are required before the system will be capable of locating such pools.			
14. SUBJECT TERMS Cone penetrometer		15. NUMBER OF PAGES 57	
		16. PRICE CODE	
17. SECURITY CLASSIFICATION OF REPORT UNCLASSIFIED	18. SECURITY CLASSIFICATION OF THIS PAGE UNCLASSIFIED	19. SECURITY CLASSIFICATION OF ABSTRACT UNCLASSIFIED	20. LIMITATION OF ABSTRACT UL

CONTENTS

1. EXECUTIVE SUMMARY

2. FIELD TEST

2.1 Background

2.2 System Hardware

2.3 Laboratory Characterization

2.4 Pre field test site visit

2.5 Field test

2.6 Discussion of results

3. SUMMARY

4. FIGURES

APPENDICIES

DECEMBER 1996 FIELD TEST OF THE FIBER OPTIC INFRARED CONE PENETROMETER

1. Executive Summary

- A two-day field test of the fiber optic infrared cone penetrometer was performed at a location near the Gulf of Mexico suspected of containing relatively shallow deposits of chlorinated solvents, especially 1,2 dichloroethane (DCA) and possibly vinyl chloride, 1,1 dichloroethane and other chlorinated complexes.
- Evidence of the presence of chlorinated DNAPLs in the soil was based on groundwater samples which showed concentration levels near the saturation limit. The sampling was at least 1 year old and just prior to the test, no direct soil samples were procured or analyzed from the exact locations at which the cone penetrometer pushes were made.
- Cone penetrometer pushes were performed at three distinct locations to depths of approximately 15 feet, limited by the 10-meter length of the IR-transmitting optical fiber cable.
- The electro-optical system comprising the infrared cone penetrometer worked nominally throughout the test and showed no degradation in performance compared to pre-test checkout in the laboratory. Recent improvements made to system hardware worked as expected.
- Laboratory characterization of system performance demonstrated the capability to detect and identify 1,2 DCA, 1,1 DCA and TCE at weight fractions greater than 2% in sample soil taken from the test site containing 20 wt% water.
- In the three locations tested, no evidence of homogeneously-distributed, free-product DNAPL in excess of 2 wt% was observed.
- In its current form, the fiber optic infrared cone penetrometer is suitable for identifying contaminants in known, saturated, free-product pools. Further performance improvements are required before the system will be capable of locating such pools.

2. FIELD TEST

2.1 Background

Recent advances in the fabrication of low-loss optical fibers which transmit infrared light has enabled the development of sensor systems for remote, in-situ infrared absorption spectroscopy. The Naval Research Laboratory is currently involved in the development of an infrared fiber optic system for the cone penetrometer. Such a system will be capable of making underground soil measurements to 1) detect and identify a wide variety of hydrocarbon contaminants, 2) determine soil clay mineralogy, and 3) determine soil water content.

The first field test of the fiber optic infrared cone penetrometer system was conducted in May 1995. Since that test, a number of hardware modifications were made to improve system performance and reliability.

NRL was given an opportunity to perform a second field test at a location near the Gulf of Mexico. (Due to possible legal issues, the exact test site is not revealed in this document and the lack of this information has no bearing on the analysis of the data and system performance.)

The purposes of this second test were: i) to demonstrate, in the field, the hardware improvements made to the system, and ii) to perform a test at a site where the confidence of obtaining a true positive result was high, that is, a site with a demonstrated DNAPL contamination plume at a depth accessible to the fiber probe.

2.2 System Hardware

A diagram of the overall sensor system is shown in Figure 1. The system consists of the probe tube with IR sensor optics, an infrared transmitting fiber optic cable for bringing light to the ground surface, and an FTIR (fourier transform infrared) spectrometer and computer housed in the push truck. In this section we will be describing in more detail several of the main features of each part of the system as well as improvements that were made since the first field trial in May 1995.

Figure 2 is a block diagram of the system showing more detail of the individual components. The penetrometer tube is fabricated out of hardened D2 tool steel and has an OD of 1.75" and in ID of 1.3". The cone tube is almost identical to the tube used for the SCAPS (Site Characterization and Penetrometer system, US Army Waterways Experiment Station) laser induced fluorescence (LIF) probe. The primary difference is the sapphire window in the side of the tube. The window used for the IR probe has been modified to allow for a greater optical throughput.

The components that make up the probe are mounted on a rail that slides into the tube and is attached with O-ring sealed screws. Figure 3 is a photograph of the rail assembly. The rail holds an IR radiation source (nichrome wire) which operates at approximately 1000K and is housed in a gold coated sphere with a sapphire window. After the radiation exits the sphere it is partially collimated by an f/1 calcium fluoride lens. The collimated light then strikes an off axis paraboloidal mirror that directs the radiation through a window in the side of the cone tube. The light is focused by this mirror to a point on the surface of the soil outside the window. A matching mirror then collects diffusely reflected light from the soil and steers this radiation through another f/1 calcium fluoride lens which in turn focuses the light onto the IR transmitting chalcogenide fiber bundle. Lastly, this light is transmitted to the FTIR spectrometer where the resulting spectrum contains information about chemical contaminants in the soil, soil type and water content.

Another important component of the sensor is a roughened gold shutter inside the probe tube in front of the window. This shutter stops radiation from reaching the soil and, more importantly, it directs a portion of the probe source radiation into the collection optics. Since this radiation is reflected from an unchanging gold reflector it gives a measure of the system transfer function and can be used for referencing and checking system performance.

Two sensor rails were aligned in the laboratory and taken into the field for this test. One rail was fitted with the optical/electrical cable and placed into a probe tube. This tube was purged with nitrogen. In the event that the probe was damaged a second tube was available and because of the modularity of the design, changing out damaged components could be accomplished quickly.

The enabling technology for this diffuse reflectance probe is the infrared transmitting optical fiber. The fibers used have been developed and fabricated at NRL and are based on chalcogenide materials (As_2S_3 , As_2Se_3 or As_2Te_3). The transmission window for these materials, depending on the exact composition, is from 2-12 μm and therefore they are appropriate for remote, in-situ IR spectroscopy. The cable used for the current field test contained a bundle of three fibers and was fabricated from core only (As_2S_3), teflon clad fiber with a core diameter of 250 μm . The minimum loss for this fibers was 0.25 dB/m at 2.4 μm and the loss at 3.4 μm was 0.27 dB/m. Figure 4 is a transmission curve for the fiber that was used. The optical cable itself is of a multilayer construction with an outer jacket of woven stainless steel. Figure 5 is a photograph of the endface of the cable showing the arrangement and size of the fibers. The cable was wrapped with expandable plastic webbing which also served to hold the electrical cable needed for the IR source power.

The FTIR spectrometer system used was a KVB/Analect RFX-40 with calcium fluoride optics operated in bistatic mode (remote IR source). The main components of the FTIR system are shown in Figure 6 and Figure 7. A short rack containing the source power supply (Kepco BOP 3606M), the FTIR electronic signal processor and controller (KVB/Analect DCM-30), and the FTIR optical interferometer (KVB/Analect TSO-40) was positioned near the push hydraulics in the truck. A 1 mm square, liquid nitrogen cooled InSb photodetector with a 5.5 μm cut-off wavelength was used. Additionally a small aperture was placed in the optical path just prior to the detector to reduce stray light. This will be explained in further detail later.

While operating, the interferometer and detector were continually purged with dry nitrogen. The computer used for controlling the system and data acquisition was located on the far side of the truck, away from the push hydraulics. Figure 8 shows the display screen of the computer during operation. This particular spectrum was recorded in the laboratory using the full system with a sample cell designed to fit the probe tube window opening. This type of cell allows controlled samples to be tested. The sample cell shown in Figure 9 contains Fisher Sea Sand contaminated with diesel fuel marine (DFM). The IR absorption due to the DFM is obvious in the spectrum.

Discussion of improvements to the system since the first field test

After the first field test at Dover Air Force Base (May 1995 - NRL Report, Fiber Optic Infrared Cone Pentrometer: Results of the May 1995 Field Test, NRL/MR/5603—96-7886) a number of areas were identified where improvements to the performance of the system could be made. In this section we will discuss those issues and how they were approached. Areas for improvement included keeping moisture out of the interferometer, reducing system noise, reducing thermal background and improving spectral referencing.

Moisture

After the May 1995 test it was discovered that the KBr optics in the FTIR interferometer had been damaged by moisture. We understood that KBr is hygroscopic and that taking the instrument in the field was risky, but counted on purging with dry nitrogen to keep moisture out. The risks of having this instrument outside were magnified by the need to open the interferometer to the atmosphere each time the instrument was moved. The main component of the interferometer is a moving wedge of KBr. Unless this wedge was manually secured for movement the wedge could move during transport and possibly damage the drive mechanism. In addition, it was rainy and humid on the days of this first field test. All this conspired to allow too much moisture into the instrument and cause the damage to the optics.

For this second generation sensor system the KBr optics in the interferometer were replaced with moisture resistant CaF_2 optics. Additionally, a sealed mechanism was designed to allow the wedge to be secured without breaking purge. Purging is still necessary to rid the system of moisture and CO_2 , but now the system is much tighter and resistant to damage from low moisture levels.

Detector Noise

For this field test we used a 1mm square InSb detector while for the May 1995 field test we used a 4mm dia InSb detector. Both these detectors had a cutoff wavelength of approximately 5.5 μm . The detector size was reduced for this test to better match the detector size to the area illuminated by the optical fiber bundle. Doing this, one would expect that the detector noise should drop with $\sqrt{\text{Area}}$. In fact, we saw no noticeable

change in the noise of the system. This suggests that the dominant source of stationary noise in the system is not the photodetector.

Thermal Background

Figure 10 is a typical spectrum of soil. Of note in this spectrum is the peak centered near 2000 cm^{-1} . This peak is due to the thermal background radiation arising from the FTIR, optics, holders and other components within the field of view of the detector through the interferometer. This energy does not contribute to the desired signal, reduced available amplifier dynamic range and reduces the band absorption features. In this section we discuss methods for minimizing this background signal.

The detector used for the system has a finite field of view (FOV) limited by a cold stop. Infrared spectrum information is carried only by radiation that has been modulated by the interferometer. The optics of the FTIR are such that the full FOV of the detector is much larger than the angular extent of light that can pass through the interferometer. Excess light that has not been modulated and still strikes the detector only effects the system if it saturates the detector. This is true because a high pass filter removes the DC level before the digitization process. What we are concerned with here though is light that is modulated, but does not originate from the output fiber of the IR probe. Figure 11 shows schematically the three major cones of radiation that strike the detector. The outer cone is the unmodulated radiation. The middle cone is stray, but modulated radiation. The final inner cone is the modulated signal light originating from the fiber bundle. Ideally, light from the source of interest (the fiber bundle) would be directed and controlled so that it matched the maximum angular extent of light passing through the interferometer. An obvious way to improve the situation is to place an aperture in front of the detector. By doing this we can dramatically decrease the background radiation while retaining the signal light. (See Figure 12.) This procedure will not eliminate the background radiation, but it will minimize the background signal relative to the desired signal.

For our particular system we placed an aperture directly on the window of the detector dewar. The aperture size was determined empirically using a variety of aperture sizes. The sensor was set up in the normal fashion and a soil sample was placed on the window. A $3.39\text{ }\mu\text{m}$ band pass filter was placed just before the fiber facet inside the cone probe. With this filter in place it possible to distinguish signal light from

background or stray radiation. Now a series of different sized apertures were placed on the detector window. With each aperture the background peak height and signal peak height were noted. This raw data is shown in Figure 13. The difference between these two numbers and ratio of these two numbers are shown respectively in Figures 14 and 15.

A different optimal aperture size is specified depending on whether one used the ratio or difference curve. Our final choice was between these two values and corresponds to the knee of the filter wavelength curve as shown in Figure 13. A final aperture diameter of 0.188" was chosen for our specific arrangement.

Improved Referencing and System Monitoring

The issues of optimal number of scans and age of reference spectrum have been explored in detail since the May 1995 field test. It was found that because of 1/f type noise the \sqrt{N} improvement with number of scans (or scan time) that would be expected in the case of white noise does not hold. After a period of time the 1/f type noise begins to dominate the system. Increasing the number of scans beyond this point degrades the spectrum. This optimal number of scans is particular to each physical setup and power level. This topic is dealt with in more detail in *Noise Characterization* below.

There is another side to the reference problem. Since over a period of time 1/f noise causes the system to drift it implies that reference spectrum "age". For maximum SNR with a referenced signal the reference should be taken at about the same time as the signal. With the original system fielded in 1995 we used a diffuse gold surface that was placed against the probe window when the probe was out of the ground. While the system was underground there was no "fresh" reference available. To address this problem a roughened gold shutter was incorporated into the design. This shutter can be seen in Figure 2. It is inside the cone tube and is operated by a cable. When it is closed over the probe window the gold scatters a portion of the source light into the collection optics and provides a constant reference. This signal can be used for determining system performance and can be used in the spectroscopic analysis of radiation diffusely scattered from soil outside the probe.

2.3 Laboratory Characterization of System

Considerable effort was spent characterizing the performance of the sensor in preparation for the field test. This section first details a system noise analysis intended to guide the selection of scan averaging number and other system operational parameters. Next, a description is given of tests of the sensor response to a variety of laboratory prepared soil samples.

Noise Characterization

Standard procedure for FTIR spectrometer operation includes averaging multiple scans into each collected spectrum. This averaging reduces the noise on the resulting measurement and hence improves achievable detection limits. However, experience, and recent research results [1] indicate that there is an optimum number of averaged scans beyond which the signal to noise ratio (SNR) of the system begins to degrade rather than improve. This behavior is due to the presence of long-term drift noise characterized by a power spectral density with low-frequency dependence of the form $1/f^\alpha$. Such noise has the property that the variance of a set of consecutive averages increases monotonically with averaging time. An experiment was performed on the field test system to determine empirically the optimum number of averaged scans.

The experiment was designed to replicate field conditions as closely as possible. The sensor was assembled in its final configuration and fitted with a sample cell filled with wet indigenous soil from the test site. The probe tip was maintained at 19° C by a chilled water recirculator to emulate conditions in the ground. Spectrum were then collected using 20, 50, 100, 200, and 500 averaged scans per spectrum. At each averaging number, ten replicate measurements were made, each measurement consisting of a gold shutter reference spectrum followed by a sample spectrum.

The data from this test were used to compute the signal to noise ratio (SNR) over the entire spectrum as a function of the number of averaged scans. Figure 16 shows the mean SNR for the reflectance spectrum formed by referencing the sample spectrum to the corresponding gold shutter references. At each averaging number, the SNR was computed as the mean over the ten replicates divided by the square root of the Allan variance. (Allan variance is the variance of the differences between consecutive replicate spectrum.) The mean was then taken over all spectral frequencies. It is clear from the figure that of the five averaging times tested the optimum SNR is achieved when 200

scans are averaged to form each spectrum. While it is possible that the true optimum may lie between 200 and 500 scans, it is not expected that the variation of SNR with averaging time is very strong in this region. Therefore it is not expected that the true optimum would yield a significant improvement over the SNR achieved at 200 scans. Further, use of more than 200 averaged scans would lead to unacceptably long data collection periods for the field test. Hence 200 scan averaging was selected for use in the field test.

Soil Sample Tests

The spectrum of a variety of laboratory prepared soil samples was measured. Due to uncertainty in the expected field conditions and target contaminants, no formal calibrations were prepared before the field test. Instead a data set was acquired which spanned the range of expected soil types, moisture contents, and contaminant species. The goal was to be prepared to make qualitative judgments in the field, reserving quantitative analysis of the data until after the test.

Soil Matrix Tests

The dominant matrix effects are soil moisture content and soil composition. The starting point for the laboratory characterization of these effects was a sample of indigenous soil collected from the test site several weeks prior to the test. Several pounds of soil were collected from the site from a depth of approximately one-foot. Analysis of the soil composition indicated 1.02% coarse sand, 35.96% fine sand, 42% silt, and 20.60% clay . The moisture content was measured to be 20 wt. % with a liquid limit of 27% and a plastic limit of 17%. The unified soil classification is CL-ML, indicating low plasticity clay, low compressibility silt. Tables 1, 2 and 3 give additional detail on the soil composition in the vicinity of the field test. The soil was mostly silty but contained stripes of clay. Two sample cells were filled with untouched indigenous soil, one from the silty section and one from a clay stripe. Figure 17 shows the spectrum of these two samples. A portion of the soil was then air dried and sieved for use in additional tests. No organic contamination of the soil was observed.

A series of samples was prepared by mixing the indigenous soil with varied proportions of fine white sand. Table 4 shows the mixtures that were prepared. All of the samples

in the table were prepared at approximately 20 wt. % water. Spectrum of these samples were collected and analyzed.

Although this data was not adequate to allow the preparation of a complete multivariate calibration set for soil composition and moisture content, it did permit identification of the major features of matrix induced variations in the spectrum. Principal Components Analysis (PCA) was used to assist in identifying these features. The clearest spectral feature correlated with variation of soil composition was the kaolinite absorption band located at 4532 cm^{-1} . Figure 18 is a example of a spectrum of sample number 2 containing 20 wt. % sand and 80 wt. % indigenous soil with 20 wt. % water. The inset in Figure 18 shows an enlargement of the kaolinite absorption band. Figure 19 is the absorbance at 4532 cm^{-1} plotted versus the weight fraction of indigenous soil in the sample. The solid curve in the figure is a logarithmic fit to the data. This information was used during the field test to determine when the probe entered soil strata of varying kaolinite composition.

Samples of indigenous soil with varying moisture content were also prepared. Spectrums were collected from these samples and variations of absorption features due to water were noted. Figure 20 shows two examples of this spectrum. Air-dried soil containing 1.3 wt. % residual water is shown with a sample with 20 wt. % water. The effects of water on the soil spectrum are pronounced. Two main effects can be identified in the figure: the overall soil albedo is reduced, and the specific water absorptions are strengthened in the wet sample. In particular the strongly saturated water absorption near 3500 cm^{-1} broadens and affects the spectrum from 2500 cm^{-1} to 3500 cm^{-1} , and the weaker water absorption at 5200 cm^{-1} also saturates and broadens.

Contaminant Tests

The infrared spectrum of soil contaminants was also examined. The contaminants of interest were chlorinated hydrocarbon solvents. Neat liquid transmission spectra of several such compounds were collected and are shown in Figure 21. Based on its anticipated presence at the test site, 1,2-Dichloroethane (1,2-DCA) was chosen as a representative compound for the preparation of soil samples. Samples containing various amounts of 1,2-DCA were prepared on indigenous soil, sand, and a mixture of 80 wt. % sand and 20 wt. % soil at various moisture contents. Figure 16 shows three examples of spectra taken from these samples. A feature due to 1,2-DCA located at 4440 cm^{-1} was

identified as the best candidate for field observation. This feature is identified in Figure 22 by a dashed vertical line. Absorptions in this region of the spectrum are relatively unaffected by moisture content and thermal background, and Figure 21 shows that several of the contaminants of interest have absorptions in this region. Based on these tests it was determined that the detection limit for 1,2-DCA on indigenous soil with 20 wt. % water is near 2 wt. %.

2.4 Pre Field Test Site Visit

Prior to the field test a site visit was made to gather information regarding soil geology, mineralogy and possible contaminants. The site under investigation is an active chemical plant that produces a variety of chlorinated hydrocarbons, chlorine, as well as a number of other products. Until recently vinyl chloride was produced at this facility as well. The primary chemical contaminants that we were looking for during the field test were 1,2 dichloroethane and 1,1 dichloroethane.

The site is located near the coast of the Gulf of Mexico. The soil is primarily fluvial river sediments with small silt stringers. In general, the clay is over consolidated and fractured. These are old deposits and looking at a cross section one can clearly see the stratification and silt stringers running at angles relative to the main layers. In this pre field test visit we were seeking information regarding the moisture content and mineralogy of the soil as well as the water table depth at the site. Prior to our visit undisturbed soil samples had been retrieved from a number of locations. From these samples we have moisture content measurements as well and mineralogical information. This data is summarized in tables 1, 2 and 3.

The water table at this site runs from 4 to 5 feet below grade. The average moisture content between the depths of 10 and 20 feet was 22.9%. The minimum value measured was 15% and the maximum value was 36%. The standard deviation on this data was 4.8% and more than 90% of the values measured were below 30%.

During the visit a sample of soil was collected from an area some distance away from the active chemical producing units, but it was felt to be representative of the whole site. By collecting this sample from a depth of 1' we insured that we were below the level of high organic content. In the laboratory, tests using a number of different

moisture contents and contamination levels were performed using the soil from the site. The results of these tests were presented above.

2.5 Field Test

When we arrived at the test site three locations at the facility had been identified as appropriate locations for pushes with our infrared probe. These locations had been investigated before and conventional cone penetrometer logs of these sites were available. These logs detailed tip and sleeve resistance as well as conductivity. Shown in Figure 23, Figure 24, and Figure 25 are copies of the tip resistance part of the logs. Overlaid on these plots are traces of the kaolinite signal recorded at each of these locations. We knew from talking to personnel on site that it was possible that we would find contaminants in the sandier layers of the soil. Samples from the clay layers had never been retrieved from these sites. With these logs an initial push site was selected and the truck was moved to that location.

After arrival at the first test site the NRL system was unloaded, assembled and operational within approximately 1.5 hours. Threading the probe tube for operation involved several steps. First the probe had to be attached to an adapter tube that connected to the smaller push pipes that were used on the cone penetrometer truck. Figure 26 shows a typical probe pipe attached to the smaller push pipe extended below the cone truck. The adapter and probe then had to be threaded through a guide that, when in place, extended from the inside the truck to just several feet below the truck floor. This guide also contained a wiper to keep soil from getting back into the truck when the probe was removed from the ground. The combination probe/adapter/guide can be seen in Figure 27 and Figure 28. Additionally, if the probe was pushed into a contaminated site a steam cleaner could be attached to this guide/wiper assembly. The next operation involved threading the optical/power cable through a number of push pipes. After this step was completed the probe was attached to the FTIR. At this point power was applied and the system was ready to be pushed into the soil. Figure 29 shows the hydraulic rams inside the truck. A push pipe and optical cable can be seen in the jaw of the rams. It should be noted that the system is quite robust. During the first assembly of the system the wiper/guide tube was being troublesome with regards to fitting into a clamping mechanism on the floor of the truck. The truck operator then used a 5 lb sledge to hammer the tube until it clicked into place. This hammering occurred approximately 3 feet from the probe itself and did no damage to the optics or alignment.

The general procedure used during the tests was as follows. The cone was pushed a known depth into the soil and the gold shutter on the probe was closed.. At this time a spectra of two hundred scans was recorded. This acted as a "fresh" reference spectra as well as confirmation of the correct operation of the probe. This number of scans had been found to yield the best SNR during laboratory tests of the system using soil from the site. Immediately after the reference spectra was recorded the shutter was open and the probe was allowed to "see" the soil. Two hundred scans were made of the reflectance spectra of the soil. This general procedure was then repeated for the next depth. On the second day of testing this procedure was modified at the last push location. At that location the number of scans for both reference and soil spectra was reduced to 100. This was done to speed operations.

To reach the full extent of the fiber optic cable it was necessary to disconnect the optical cable from the FTIR after about 10 feet. While it was disconnected additional push pipes were threaded onto the system. After the additional pipes were added the cable was reconnected to the FTIR and the push continued. With the gold shutter system it was possible to tell immediately that the disconnect/reconnect procedure did not effect return signal levels.

Periodically, the IR detector was refilled with liquid nitrogen and the nitrogen purge gas that flowed through the interferometer and detector was checked.

2.6 Discussion of Field Test Results

Hardware Performance

The system performance throughout the field test was excellent. The inclusion of a gold reference shutter in the optical design allowed continuous monitoring of the optical throughput and instrument response function. The optical throughput was stable at the same levels observed in pre-test measurements and remained unchanged after two days of field testing. No alignment or adjustment of the optical system was required at any time during the field test. The instrument response function remained unchanged throughout the field test.

After first setting up, significant noise was observed in the final spectral output. This noise, believed to be due to truck vibrations, was eliminated by simply repositioning the rack containing the FTIR spectrometer.

Slow variation of the thermal background corresponding to diurnal temperature fluctuation was observed in the field test data. As expected, these variations were more pronounced in the field than in the laboratory. The expected subtle changes in instrument response due to periodic re-supply of detector coolant were also observed in the field test reference spectra.

Mineralogy

Variations of soil mineralogy with depth were clearly observed during the field test. The kaolinite absorption band described above was observed in the field. Variations of this band were used to establish when the sensor was in sand versus clay. Figures 23,24 and 25 show the variation of the kaolinite absorption band-depth as a function of sensor depth for the three test sites. Also shown is the tip pressure log of an earlier CPT push at the same location. Increases in tip pressure correspond to sand layers in the soil. The figures show good agreement between the CPT log and the kaolinite band-depth.

A weaker absorption band was also observed near 4360 cm^{-1} during the field test. One possible source of this absorption is smectite clay. Figure 30 shows field data with this feature overlaid with a laboratory spectrum of ferruginous smectite clay, which has an absorption near 4367 cm^{-1} . The laboratory smectite sample is from Grant County, Washington, USA, and was obtained through the University of Missouri-Columbia, Source Clay Minerals Repository (marked SWa-1). Another possible source for this absorption is discussed below.

Absence of Chlorinated Solvents

During the two-day test period, over 100 data files were recorded corresponding to various depths at the three push locations. None of the data indicated the presence of free product chlorinated solvents (TCE, 1,1 DCA, or 1,2 DCA) at levels exceeding approximately 2 wt%. In this section, we discuss possible reasons for this observation.

Evidence for the types and levels of contamination at the three sites chosen came indirectly from historical data and from laboratory analysis of groundwater performed in years past. In the case of groundwater analysis for two of the three sites, it was found that the water contained saturated levels of dissolved 1,1 DCA and 1,2 DCA and thus it was concluded that free product DNAPL had existed in the immediate area. It must be emphasized strongly that prior to the tests using the fiber optic cone penetrometer, to our knowledge, no soil samples were extracted and analyzed from the exact locations and depths at which pushes were made using the fiber system. Hence, no direct evidence existed for the presence of free product DNAPL at these locations at the time the fiber system was tested. Throughout the test, it was possible to perform reference checks on the operation of the fiber optic system using the newly-installed movable gold reflector. It was verified that the optical system performed nominally in the field with no degradation compared to performance in the laboratory. Furthermore, laboratory tests (see Fig. 22) verified the capability of the fiber optic system to detect and identify 1,2 DCA at levels in excess of 2 wt % in soil of the same type and water content as encountered at the three test sites. Hence, we conclude that, at the exact depths and locations at which measurements were made, there was no DNAPL contamination in excess of 2 wt %. This is not to say that free product DNAPL was not present at adjacent locations, perhaps even at locations within a few meters of the push locations. Just as with LIF measurements using the cone penetrometer, the infrared reflectance sensor performs essentially a point measurement and samples a soil volume of at most a few cubic millimeters, depending on soil type, water content, and compaction level. However, based on laboratory results, it is clear that the system will, without ambiguity, identify the contents of DNAPL-saturated plumes for any soil type and water content.

It is still possible that free product pools of DNAPL were present nearby to the locations tested but were not detected. This well-known problem stems from the statistical probability of encountering such a pool using a SCAPS approach. As pointed out by Pankow and Cherry, Dense Chlorinated Solvents and other DNAPLS in Groundwater, Waterloo Press, 1996, pp. 65 "In field investigations of sites where extensive solvent contamination exists, pools of free-product solvent are found only rarely, even when their existence is not in doubt. Such accumulation zones are rarely found because conventional site investigation techniques are not well-suited for their detection, and because drilling and sampling the large number of boreholes necessary to encounter small to medium size pools is usually not practical."

Free product DNAPL can also exist underground in the form of ganglia or microglobules. In this case, the spatial distribution of DNAPL is extremely heterogeneous and an optical point probe will have an extreme disadvantage compared to methods which, for example, draw gas, liquid, or solid sample from a much larger volume either for in-situ analysis or for transport to the surface for analysis.

Therefore, we conclude that the absence of spectral evidence of DANPL-saturated soil at the three locations tested represents a "true negative" result at the level of 2 wt%. However, in order to serve as a useful tool for locating unknown DNAPL pools and ganglia in arbitrary soil types and moisture levels, significant system performance improvements must be made to the fiber optic infrared cone penetrometer.

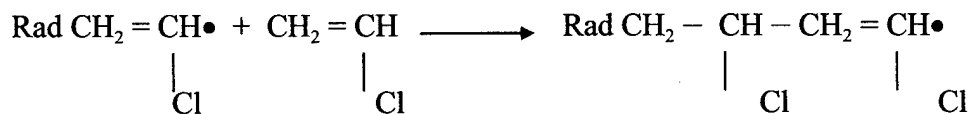
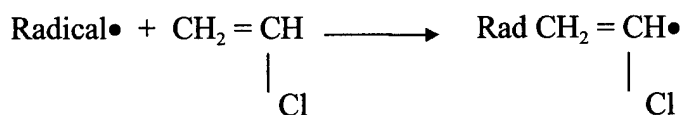
Possible Observation of Polyvinyl Chloride in Clay

Several absorption features were observed in the field test data that are still not positively identified. These features appear near 4360 cm^{-1} , 2960 cm^{-1} , 2910 cm^{-1} , and 2850 cm^{-1} . As noted in an earlier section, the feature at 4360 cm^{-1} may be due to smectite clay. However, the data is also consistent with the presence of low molecular weight Polyvinyl Chloride (PVC) in the soil. Figure 31 and Figure 32 show the spectra in the two regions affected. Figure 31 shows a field test spectrum from push 2 at a depth of 6' 5" compared to a laboratory prepared sample of 9 wt% powdered low molecular weight PVC on indigenous soil with 23 wt. % water, both in the region of the 4360 cm^{-1} absorption. Note that the PVC gives rise to an absorption near 4360 cm^{-1} . Figure 32 shows reflectance spectra from the same push at a depth of 2' 4" compared to a sample of pure PVC, both in the region of 2900 cm^{-1} . In this figure the pure PVC spectrum has been shifted 55 cm^{-1} to allow comparison of the three absorption peaks. Again there appears to be some consistency. Note that in both spectral regions the absorptions observed in the field and the candidate PVC absorptions disagree by approximately 30-60 cm^{-1} . However, the locations of the absorption peaks of PVC vary by similar amounts as a function of the molecular weight.

Vinyl chloride was manufactured at the site in question in the relatively recent past. Further it is believed that there was at one time buried pipeline at the location of this push at a depth of approximately 6' - 7'. All of this information is consistent with the possible release of vinyl chloride into the soil. However, vinyl chloride exists as a gas at ambient temperatures (bp = -13.4°C). Therefore the question is how could any vinyl

chloride spilled in the past remain in the oil for detection by the IR cone penetrometer probe?

Production of polyvinyl chloride is prepared by free radical polymerization of vinyl chloride as outlined below [2]:



In this reaction the peroxide is used to form a free radical which adds to the double bond of the monomer initiates the growth of the polymer. The free radical formed by the reaction between the peroxide radical and the monomer can react with another monomer molecule which forms a longer chain radical, which in turn can react further. The key part of this reaction is the free radical initiation of the polymerization. It has been shown by Soma, et al [3], that when aromatic compounds are absorbed by clay such as montmorillonite, the colored species are formed. The colored species formed were identified by ESR and Raman spectroscopy as aromatic cation radicals. The presence of these radicals in the clay could act as an initiator for the in-situ polymerization of the vinyl chloride. Indeed, King et al [4] have demonstrated that toluene is polymerized when sorbed into clay. Therefore, it is not unlikely that when a large amount of vinyl chloride is spilled into a clay bearing soil that radical polymerization, initiated either by the clay or organics contained in the clay, can occur. Therefore, the bands in the 2900 cm-1 region could be attributed to the presence of polyvinyl chloride which resulted from the clay initiated polymerization of spilled vinyl chloride

3.0 Summary

A two-day field test of the fiber optic infrared cone penetrometer was performed at a location near the Gulf of Mexico suspected of containing relatively shallow deposits of chlorinated solvents, especially 1,2 dichloroethane(DCA) and possibly vinyl chloride, 1,1 dichloroethane and other chlorinated complexes.

Cone penetrometer pushes were performed at three distinct locations to depths of approximately 15 feet, limited by the 10 meter length of the IR-transmitting optical fiber cable. The electro-optical system comprising the infrared cone penetrometer worked nominally throughout the test and showed no degradation in performance compared to pre-test checkout in the laboratory. Recent improvements made to system hardware worked as expected. Laboratory characterization of system performance demonstrated the capability to detect and identify 1,2 DCA, 1,1 DCA and TCE at weight fractions greater than 1% in sample soil taken from the test site containing 20 wt% water.

In the three locations tested, no evidence of homogeneous, free-product DNAPL saturated soil in excess of 2 wt% was observed. In order to serve as a useful tool for locating unknown DNAPL pools and ganglia in arbitrary soil types and moisture levels, significant system performance improvements must be made to the fiber optic infrared cone penetrometer.

References

1. G. Hazel, F. Bucholtz, I.D. Aggarwal, " Characterization and modeling of drift noise in Fourier transform spectroscopy: implications for signal processing and detection limits", *Appl Opt.*, Sept 1997, V 36, No 27, pp 6751-6759.
2. R.T. Morrison and R.N. Boyd, *Organic Chemistry*, 3rd Edition, p. 1030 (Allyn and Bacon Inc, 1975).
3. Soma, Y. Soma, M; Harada, I Formation of aromatic cations in the interlayer of monomorillonites studied by resonance Raman spectroscopy, *Proc. IX International Conference on Raman Spectroscopy*, p. xxxvi+894, 648-9
4. T. King, Private communications

5. **4.0 Tables and Figures**

Depth (feet bgs)	Quartz (volume %)	Feldspar (volume %)	Carbonate (volume %)	Total Clay (volume %)
30.1	41	6	0	53
35.1	18	9	0	73
40.2	56	1	0	43
45.3	18	11	0	71
50.5	61	10	0	59
54.4	10	4	0	86
65.6	43	6	0	51

Table 1. Typical Bulk Mineralogy

Depth (feet bgs)	Total Clay (volume %)	Illite (volume %)	Kaolinite (volume %)	Chlorite (volume %)	Smectite (volume %)
30.1	53	10	5	0	38
35.1	73	15	8	0	50
40.2	43	6	2	1	34
45.3	71	15	6	0	50
50.5	59	12	4	0	43
54.4	86	15	4	1	66
65.6	51	10	3	0	38

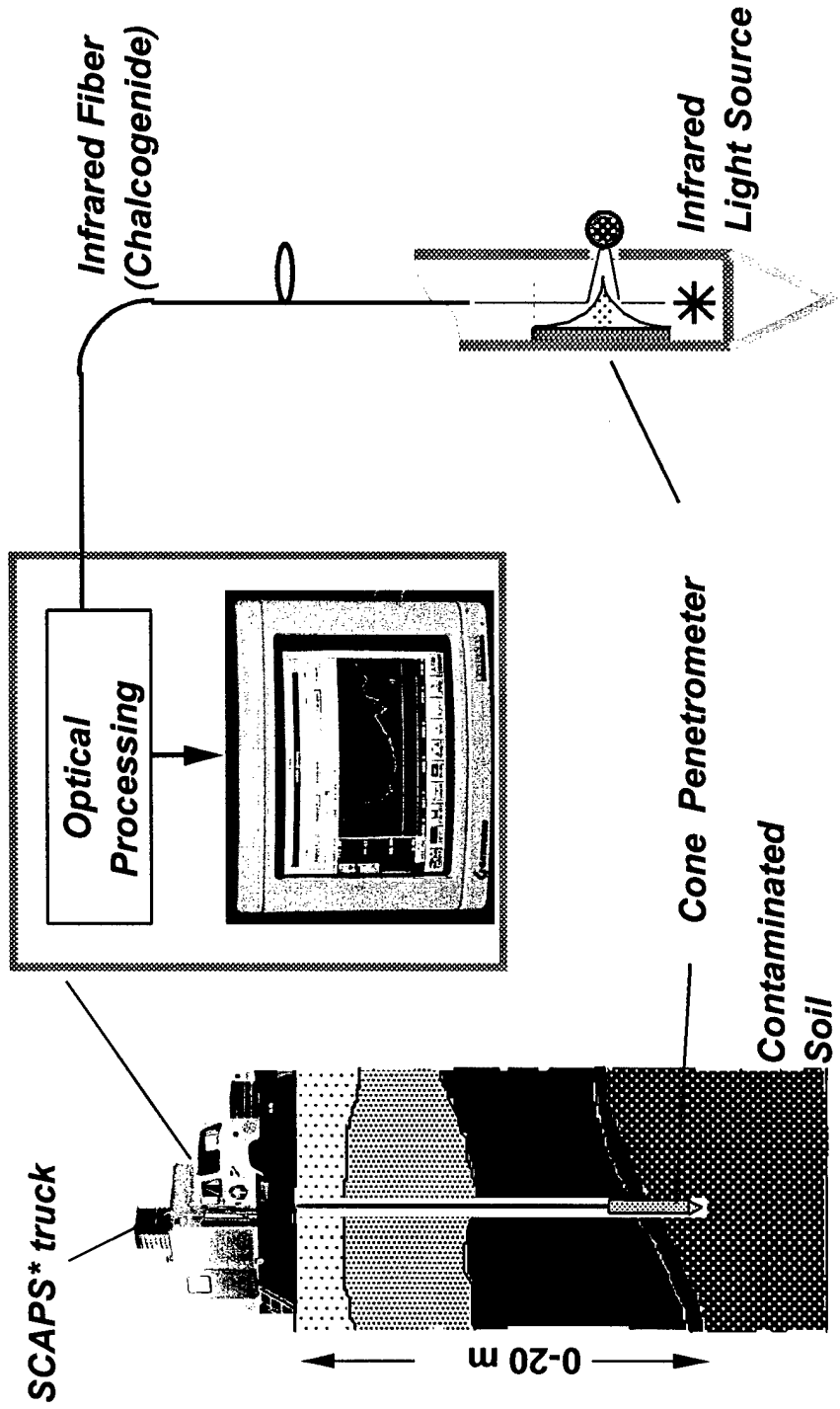
Table 2. Typical Clay Mineralogy

Well ID	Depth	Moisture Content
94M017-120	11	35
95DP-25-140	10	18
95DP-25-140	15	18
95DP-25-140	20	15
94M002-80	10	21
94M002-80	12	24
94M002-80	12	25
94M003-80	10	22
94M004-80	11	18
94M004-80	12	25
94M007-80	16	20
94M008-80	10	17
94M008-80	14	18
94M020-S	10	19
94M020-S	12	28
CW02-200D	10	21
CW02-200D	16	25
CW004-200	12	26
CW007-200	10	27
CW009-200	11	18
CW009-200	13	221
CW011-200	11	20
Z4E030	11	26
Z4E030	13	26
Z4E031	14	26
Z4E032	14	24
Z4E017	12	20
Z4E017	16	25
Z5G002	19	17.8
Z5G002	19	19
Z5G004	16	26
Z5G004	18	28
Z5G005	12	23
Z5G005	16	36
Z5G006	18	23

Table 3. Water content at a number of sites.

Sample Number	Sample Composition	
	Weight Fraction Sand (%)	Weight Fraction Soil (%)
1	0	100
2	20	80
3	50	50
4	80	20
5	100	0

Table 4: Samples prepared for characterization of sensor response to varying soil composition.



* (Site Characterization and Analysis Penetrometer System)

Figure 1. Schematic of overall system.

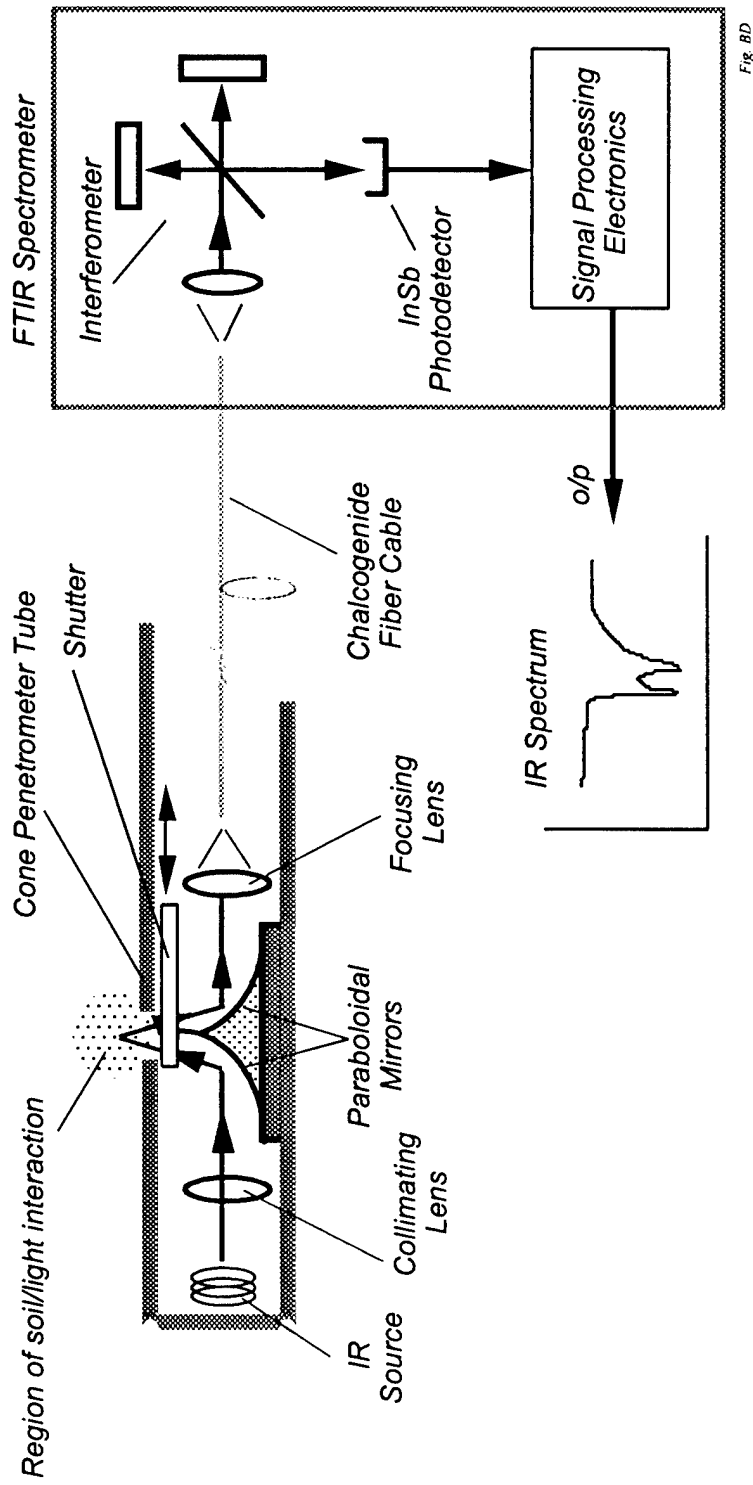


Fig. BD

Figure 2. Schematic of sensor.

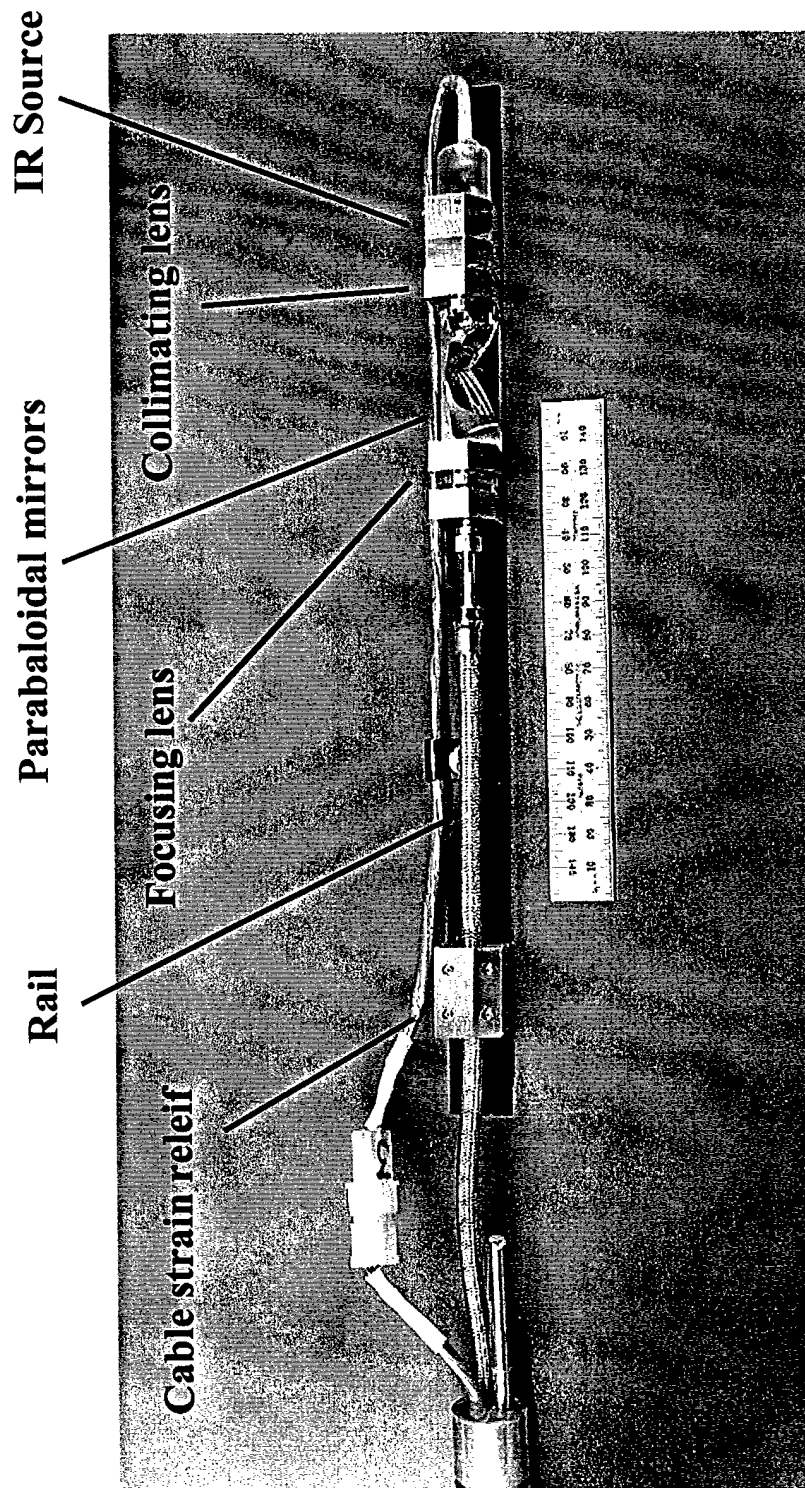


Figure 3. Photograph of rail assembly.

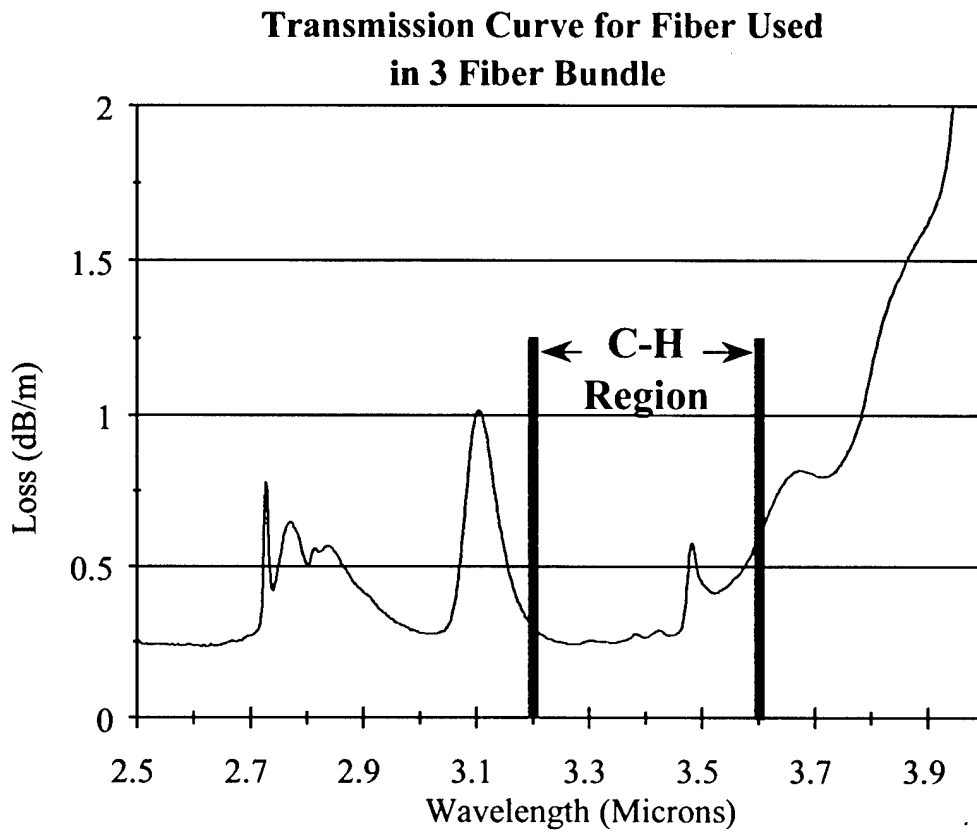


Figure 4. Transmission curve for chalcogenide fibers used in cable.

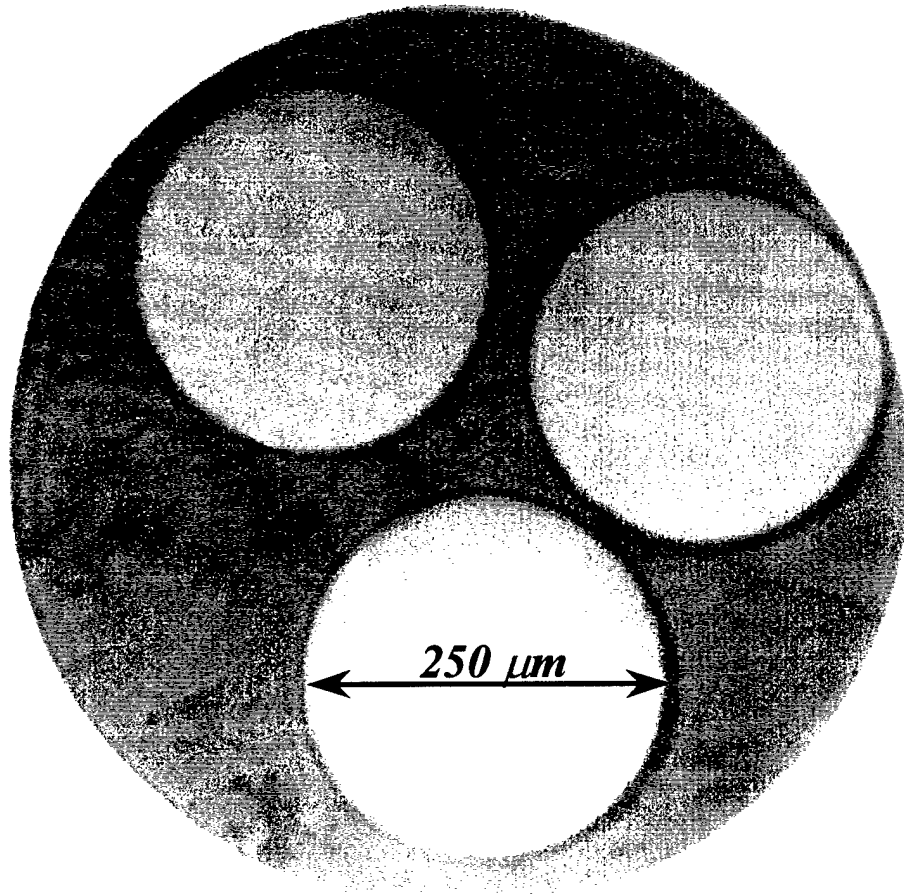


Figure 5. Photograph of the endface of the 3-fiber cable showing the three infrared-transmitting chalcogenide fibers.

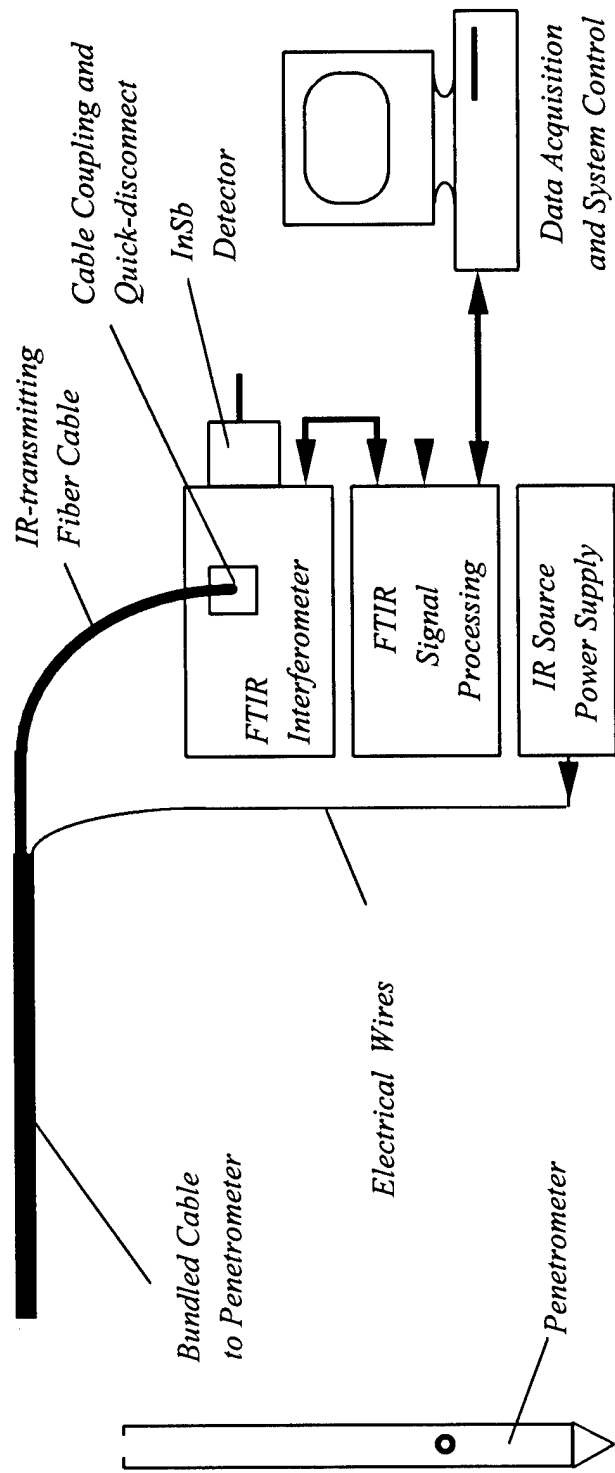


Fig. 1B

Figure 6. Block diagram of instrumentation.

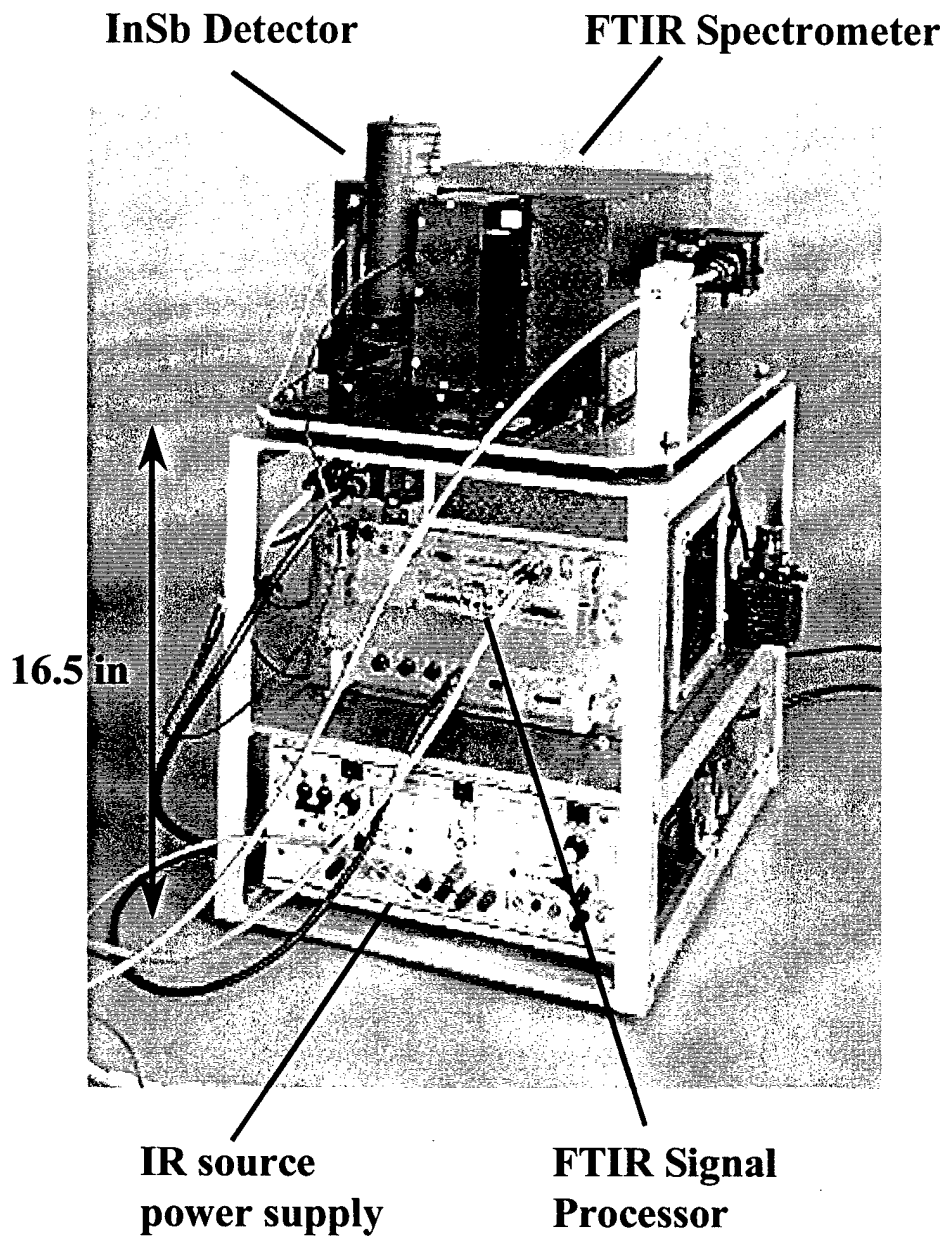
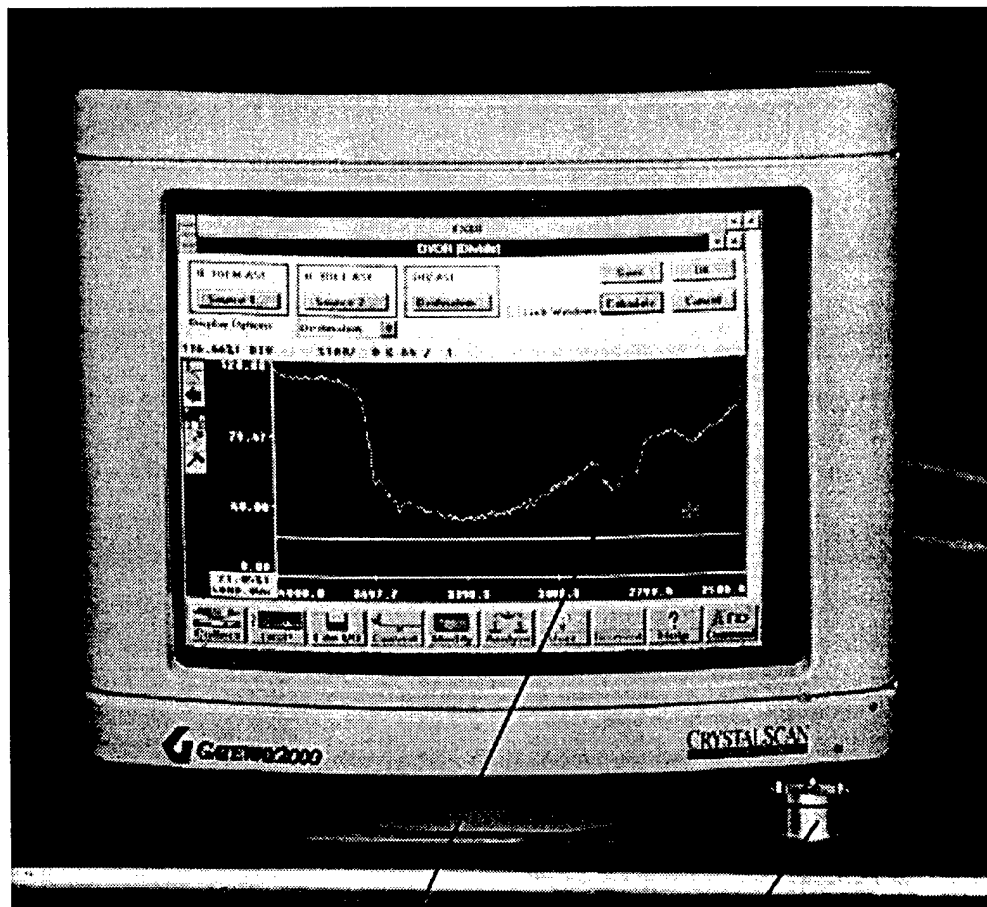


Figure 7. Rack assembly showing the instrumentation components illustrated in Figure 6.



Penetrometer tube

Sample cell

C-H stretch absorption feature

Fig. 8. IR spectrometer display panel. Spectrum shown was obtained with a sample cell containing a soil-hydrocarbon(DFM) mixture attached to the penetrometer tube.